

# Effective masses of diquarks

P. Maris\*

Dept. of Physics, North Carolina State University, Raleigh, NC 27695-8202

October 24, 2018

## Abstract

We study meson and diquark bound states using the rainbow-ladder truncation of QCD's Dyson–Schwinger equations. The infrared strength of the rainbow-ladder kernel is described by two parameters. The ultraviolet behavior is fixed by the one-loop renormalization group behavior of QCD, which ensures the correct asymptotic behavior of the Bethe–Salpeter amplitudes and brings important qualitative benefits. The diquark with the lowest mass is the scalar, followed by the axialvector and pseudoscalar diquark. This ordering can be anticipated from the meson sector.

## 1 Introduction

Mesons are color-singlet bound states of a quark and an antiquark. In addition to quark-antiquark bound states, one could also ask the question whether or not there are quark-quark bound states, by studying the corresponding Bethe–Salpeter equation [BSE] for bound states. Such states are of course not colorless in QCD, and are therefore expected to be confined, if they exist at all. Nevertheless, the masses of these states can serve as an indication for the relevant mass scales of quark-quark correlations. Such diquark correlations could play a role inside baryons: two quarks bound in a color antitriplet configuration can couple with a quark to form a color-singlet baryon. Indeed, recent studies of baryons as bound states of a quark and a (confined) diquark are quite successful in describing baryons [1, 2, 3, 4]. Also some lattice simulations [5] indicate the existence of correlations in diquark channels.

Here we report ground state meson and color-antitriplet diquark masses based on the rainbow-ladder truncation of the set of Dyson–Schwinger equations [DSEs] [6, 7]. This covariant approach accommodates quark confinement and implements QCD's one-loop renormalization group behavior. The model we apply has previously been shown to give an efficient description of the masses and electroweak decay constants of the light pseudoscalar and vector mesons [8, 9] and their interactions [10, 11, 12, 13]. This calculation will provide information

---

\**E-mail address:* pmaris@unity.ncsu.edu

to guide the improvement of quark-diquark models of baryons and assists in developing an intuitive understanding of lattice simulations.

## 2 Dyson–Schwinger Equations

The DSE for the renormalized quark propagator in Euclidean space is

$$S(p)^{-1} = i Z_2 \not{p} + Z_4 m_q(\mu) + Z_1 \int_q^\Lambda g^2 D_{\mu\nu}(k) \frac{\lambda^i}{2} \gamma_\mu S(q) \Gamma_\nu^i(q, p), \quad (1)$$

where  $D_{\mu\nu}(k = p - q)$  is the dressed-gluon propagator,  $\Gamma_\nu^i(q, p)$  the dressed-quark-gluon vertex with color-octet index  $i = 1, \dots, 8$ , and  $Z_2$  and  $Z_4$  are the quark wave-function and mass renormalization constants. The notation  $\int_q^\Lambda \equiv \int^\Lambda d^4q / (2\pi)^4$  stands for a translationally invariant regularization of the integral, with  $\Lambda$  being the regularization mass-scale. The regularization is removed at the end of all calculations, by taking the limit  $\Lambda \rightarrow \infty$ . We use the Euclidean metric where  $\{\gamma_\mu, \gamma_\nu\} = 2\delta_{\mu\nu}$ ,  $\gamma_\mu^\dagger = \gamma_\mu$  and  $a \cdot b = \sum_{i=1}^4 a_i b_i$ . The most general solution of Eq. (1) has the form  $S(p)^{-1} = i\not{p}A(p^2) + B(p^2)$  and is renormalized at spacelike  $\mu^2$  according to  $A(\mu^2) = 1$  and  $B(\mu^2) = m_q(\mu)$  with  $m_q(\mu)$  being the current quark mass.

### 2.1 Meson Bethe–Salpeter Equation

Mesons are color-singlet quark-antiquark bound states. They are solutions of the homogeneous Bethe–Salpeter equation [BSE] for  $q\bar{q}$  bound states

$$\Gamma_M^{\alpha\beta}(p_+, p_-) \delta_{ab} = \int_q^\Lambda K_{ac;db}^{\alpha\gamma;\delta\beta}(p_+, q_+; q_-, p_-) S^{\gamma\gamma'}(q_+) \Gamma_M^{\gamma'\delta'}(q_+, q_-) \delta_{cd} S^{\delta'\delta}(q_-), \quad (2)$$

where  $p_+ = p + \eta P$  and  $p_- = p - (1 - \eta)P$  are the outgoing and incoming quark momenta respectively, and  $q_\pm$  is defined similarly, see also Fig. 1. The

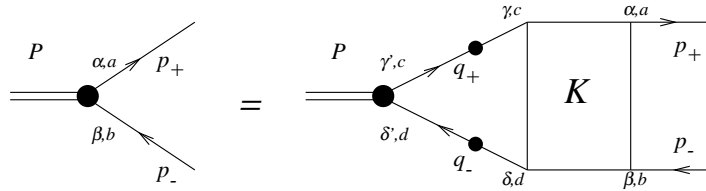


Figure 1: Meson Bethe–Salpeter Equation.

greek superscripts are spinor indices, and the roman subscripts are color indices running from 1 to 3; for simplicity we consider one flavor here. The kernel

$K$  is the renormalized, amputated  $q\bar{q}$  scattering kernel that is irreducible with respect to a pair of  $q\bar{q}$  lines.

This equation has solutions at discrete values of  $P^2 = -m_M^2$ , where  $m_M$  is the meson mass. Together with the canonical normalization condition for  $q\bar{q}$  bound states, it completely determines  $\Gamma_M$ , the bound state Bethe–Salpeter amplitude [BSA]. The different types of mesons, such as pseudo-scalar, vector, etc. are characterized by different Dirac structures. The most general decomposition for pseudoscalar bound states is

$$\begin{aligned} \Gamma_{PS}(q_+, q_-) = & \gamma_5 [iE(q^2, q \cdot P; \eta) + \not{P} F(q^2, q \cdot P; \eta) \\ & + \not{k} G(q^2, q \cdot P; \eta) + \sigma_{\mu\nu} P_\mu q_\nu H(q^2, q \cdot P; \eta)], \end{aligned} \quad (3)$$

where the invariant amplitudes  $E$ ,  $F$ ,  $G$  and  $H$  are Lorentz scalar functions of  $q^2$  and  $q \cdot P$ . Note also that these amplitudes explicitly depend on the momentum partitioning parameter  $\eta$ . However, so long as Poincaré invariance is respected, the resulting physical observables are independent of this parameter [8, 10]. If  $\eta = \frac{1}{2}$ , these amplitudes are appropriately odd or even in the charge parity odd quantity  $q \cdot P$  for charge eigenstates. In the case of the  $0^{-+}$  pion, for example, the amplitude  $G$  is odd in  $q \cdot P$ , the others are even.

The most general decomposition for scalar mesons can be obtained from that for a pseudoscalar mesons by dropping the  $\gamma_5$ . For the  $0^{++}$ , the amplitude  $F$  is odd in  $q \cdot P$ , the others are even, if we use the same notation as for the pseudoscalars. A vector meson has more Dirac structures: a massive vector meson being transverse, the general decomposition of a such a BSA requires eight covariants [9], the dominant structure being

$$\Gamma_\mu^{\text{dom}}(q_+, q_-) = \left( \delta_{\mu\nu} - \frac{P_\mu P_\nu}{P^2} \right) \gamma_\nu V_1(q^2, q \cdot P; \eta). \quad (4)$$

For the  $1^{--}$   $\rho$  meson, the function  $V_1(q^2, q \cdot P; \eta = \frac{1}{2})$  is even in  $q \cdot P$ .

## 2.2 Diquark bound states

Diquarks are quark-quark correlations. In QCD, with  $N_c = 3$ , these states are necessarily colored and therefore believed to be confined. Two quarks can be coupled in either a color sextet or a color antitriplet. Single gluon exchange leads to an (effective) interaction that is attractive for diquarks in a color antitriplet configuration, but the interaction is repulsive in the color sextet channel [14, 15]. Furthermore, it is the diquark in a color antitriplet that can couple with a quark to form a color-singlet baryon. Thus we will only consider in diquarks in a color antitriplet configuration.

Using the antisymmetric tensor  $\epsilon_{abc}$  as a representation of the antitriplet [16], the corresponding diquark bound states can be described by solutions of the homogeneous BSE

$$\begin{aligned} \Gamma_D^{\alpha\beta}(p_+, -p_-)\epsilon_{abc} = & \int_q^\Lambda K_{ad;be}^{\alpha\gamma;\beta\delta}(p_+, q_+; -p_-, -q_-) \\ & S^{\gamma\gamma'}(q_+) \Gamma_M^{\gamma'\delta'}(q_+, -q_-) \epsilon_{dec} S^{\delta\delta'}(-q_-), \end{aligned} \quad (5)$$

where  $p_+ = p + \eta P$  and  $-p_- = -p + (1 - \eta)P$  are now *both outgoing* quark momenta (and similarly for  $q_+$  and  $-q_-$ ). This is schematically depicted in Fig. 2; note the difference in the argument and the order of the indices of the second quark propagator and of the kernel  $K$  compared to the meson BSE, Eq. (2). With the help of the charge conjugation matrix  $C$ , which satisfies

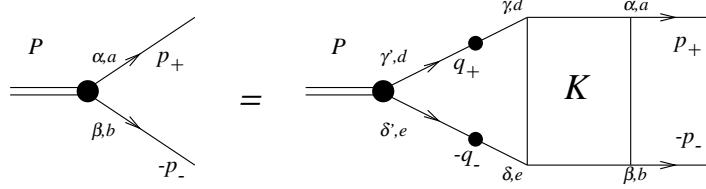


Figure 2: Diquark Bethe–Salpeter equation.

$C^2 = -1$  and  $C \gamma_\mu C = (\gamma_\mu)^T$ , we can rewrite the BSE for diquarks as [14]

$$\begin{aligned} \left( \Gamma_D(p_+, -p_-) C \right)^{\alpha\beta'} \epsilon_{abc} &= -\epsilon_{dec} \int_q^\Lambda K_{ad;be}^{\alpha\gamma;\beta\delta}(p_+, q_+; -p_-, -q_-) C^{\delta''\delta} C^{\beta\beta'} \\ &S^{\gamma\gamma'}(q_+) \left( \Gamma_D(q_+, -q_-) C \right)^{\gamma'\delta'} S(q_-)^{\delta'\delta''}. \end{aligned} \quad (6)$$

This equation resembles the meson BSE; in fact, using a skeleton expansion of the kernel  $K$  one can show that  $\Gamma_D(q_+, -q_-)C$  satisfies a BSE whose Dirac structure is identical to that of the meson BSE for  $\Gamma_M(q_+, q_-)$ . Only its color structure is different, and that has important consequences [17].

As in the case of mesons, the different types of diquarks are characterized by different Dirac structures. Since the intrinsic parity of a quark-quark pair is opposite to that of a quark-antiquark pair, a scalar diquark BSA, or rather  $\Gamma_{D,\text{scal}}(q_+, -q_-)C$ , has exactly the same form as a pseudoscalar meson BSA, Eq. (3). Similarly, an axialvector diquark BSA has the same decomposition as a vector meson BSA, and a pseudoscalar diquark BSA has the same form as a scalar meson BSA.

### 2.3 Two-body bound states in rainbow-ladder truncation

For practical calculations, we utilize the rainbow truncation of the quark DSE

$$Z_1 g^2 D_{\mu\nu}(k) \Gamma_\nu^i(q, p) \rightarrow \mathcal{G}(k^2) D_{\mu\nu}^{\text{free}}(k) \gamma_\nu \frac{\lambda^i}{2}, \quad (7)$$

in combination with the ladder truncation of the BSE

$$\begin{aligned} K_{ac;db}^{\alpha\gamma;\delta\beta}(p_+, q_+; q_-, p_-) &\rightarrow \\ -\mathcal{G}(k^2) \left( \frac{\lambda^i}{2} \right)_{ac} (\gamma_\mu)^{\alpha\gamma} D_{\mu\nu}^{\text{free}}(k) \left( \frac{\lambda^i}{2} \right)_{db} (\gamma_\nu)^{\delta\beta}, \end{aligned} \quad (8)$$

where  $D_{\mu\nu}^{\text{free}}(k = p - q = p_{\pm} - q_{\pm})$  is the free gluon propagator in Landau gauge. These two truncations are consistent in the sense that the combination produces vector and axialvector vertices satisfying the respective Ward–Takahashi identities [8]. In the axial case, this ensures that in the chiral limit the ground state pseudoscalar mesons are the massless Goldstone bosons associated with chiral symmetry breaking; with nonzero current quark masses it leads to a generalization of the Gell-Mann–Oaks–Renner relation [18]. In the vector case, this ensures conservation of the electromagnetic current [10].

If we insert this ladder kernel, Eq. (8), in the meson BSE, we get the ladder BSE for the meson BSA

$$\Gamma_M^{\alpha\beta}(p_+, p_-) = -\frac{1}{3} \text{Tr}_c \left[ \frac{\lambda^i}{2} \frac{\lambda^i}{2} \right] \int_q^{\Lambda} \mathcal{G}(k^2) D_{\mu\nu}^{\text{free}}(k) \left( \gamma_{\mu} S(q_+) \Gamma_M(q_+, q_-) S(q_-) \gamma_{\mu} \right)^{\alpha\beta}, \quad (9)$$

For the diquark bound states we obtain

$$\left( \Gamma_D(p_+, -p_-) C \right)^{\alpha\beta} \epsilon_{abc} = \epsilon_{dec} \left( \frac{\lambda^i}{2} \right)_{ad} \left( \frac{\lambda^i}{2} \right)_{be} \int_q^{\Lambda} \mathcal{G}(k^2) D_{\mu\nu}^{\text{free}}(k) \left( \gamma_{\mu} S(q_+) \Gamma_D(q_+, -q_-) C S(q_-) \gamma_{\mu} \right)^{\alpha\beta}. \quad (10)$$

Comparing Eq. (9) with Eq. (10), we see that in ladder truncation the only difference between the meson BSE for  $\Gamma_M$  and BSE for a color-antitriplet diquark, or rather, for  $\Gamma_D C$ , lies in the color factors. For the mesons, we have  $\text{Tr}_c[\frac{\lambda^i}{2} \frac{\lambda^i}{2}] = 4$ , and thus we get a factor of  $-4/3$  in front of the BSE integral. For the diquarks in a color antitriplet configuration on the other hand, we have

$$\left( \frac{\lambda^i}{2} \right)_{ad} \left( \frac{\lambda^i}{2} \right)_{be} \epsilon_{dec} = -\frac{2}{3} \epsilon_{abc}. \quad (11)$$

Thus, in *ladder truncation* the effective interaction for the diquarks is reduced by a factor of two compared to the interaction in the meson channel. Beyond ladder truncation a more complex algebraic relation persists between the meson and diquark BSEs [17]. We therefore expect that the diquarks with the lowest mass are the scalar diquarks (the diquark partners of the pseudoscalar mesons), followed by the axialvector and pseudoscalar diquarks [14].

The rainbow-ladder truncation is particularly suitable for the flavor octet pseudoscalar mesons and for the vector mesons, since the next-to-leading-order contributions in a quark-gluon skeleton graph expansion have a significant amount of cancellation between repulsive and attractive corrections [17, 19]. However, the BSE for diquarks, and also the scalar meson BSE, receive large repulsive corrections from these next-to-leading-order contributions. This will significantly change the scalar meson mass and corresponding BSA; the diquark bound states found in ladder truncation will in fact disappear altogether from the spectrum [17, 19, 20]. Nevertheless, correlations will persist in the diquark channels and diquark masses found in ladder truncation can serve as a guide for parametrizing those correlations.

### 3 Numerical calculations

#### 3.1 Model interaction

For our numerical calculations we employ a model for the effective coupling  $\mathcal{G}(k^2)$  that has been developed through an efficient description of the masses and decay constants of the light pseudoscalar and vector mesons [9]. This effective  $\bar{q}q$  interaction is constrained by perturbative QCD in the ultraviolet and has a phenomenological infrared behavior. The form is

$$\frac{\mathcal{G}(k^2)}{k^2} = \frac{4\pi^2 D k^2}{\omega^6} e^{-k^2/\omega^2} + \frac{4\pi^2 \gamma_m \mathcal{F}(k^2)}{\frac{1}{2} \ln \left[ \tau + (1 + k^2/\Lambda_{\text{QCD}}^2)^2 \right]}, \quad (12)$$

with  $\gamma_m = 12/(33 - 2N_f)$  and  $\mathcal{F}(s) = (1 - \exp \frac{-s}{4m_t^2})/s$ . The ultraviolet behavior is chosen to be that of the QCD running coupling  $\alpha(k^2)$ ; the ladder-rainbow truncation then generates the correct perturbative QCD structure of the DSE-BSE system of equations. The first term implements the strong infrared support in the region  $0 < k^2 < 1 \text{ GeV}^2$  phenomenologically required [21] to produce a realistic value for the chiral condensate. We use  $m_t = 0.5 \text{ GeV}$ ,  $\tau = e^2 - 1$ ,  $N_f = 4$ ,  $\Lambda_{\text{QCD}} = 0.234 \text{ GeV}$ , and a renormalization scale  $\mu = 19 \text{ GeV}$  which is well into the perturbative domain [8, 9]. The remaining parameters,  $\omega = 0.4 \text{ GeV}$  and  $D = 0.93 \text{ GeV}^2$  along with the quark masses, are fitted to give a good description of the chiral condensate,  $m_{\pi/K}$  and  $f_\pi$ .

Within this model, the quark propagator reduces to the one-loop perturbative QCD propagator in the ultraviolet region. In particular, the dynamical mass function  $M(p^2) = B(p^2)/A(p^2)$  behaves like

$$M(p^2) \simeq \frac{\hat{m}_q}{\left( \frac{1}{2} \ln \left[ \frac{p^2}{\Lambda_{\text{QCD}}^2} \right] \right)^{\gamma_m}}, \quad (13)$$

where  $\hat{m}_q$  is the renormalization-point-independent explicit chiral-symmetry-breaking mass. In the chiral limit the behavior is qualitatively different

$$M_{\text{chiral}}(p^2) \simeq \frac{2\pi^2 \gamma_m}{3} \frac{-\langle \bar{q}q \rangle^0}{p^2 \left( \frac{1}{2} \ln \left[ \frac{p^2}{\Lambda_{\text{QCD}}^2} \right] \right)^{1-\gamma_m}}, \quad (14)$$

with  $\langle \bar{q}q \rangle^0$  the renormalization-point-independent chiral condensate [8]. Its relation to the renormalization-dependent condensate

$$\langle \bar{q}q \rangle^\mu = -3 Z_4 \int_q^\Lambda \text{Tr}[S_{\text{chiral}}(p)], \quad (15)$$

is at one-loop level

$$\langle \bar{q}q \rangle^\mu = (\ln \mu / \Lambda_{\text{QCD}})^{\gamma_m} \langle \bar{q}q \rangle^0. \quad (16)$$

As demonstrated clearly in Ref. [18], this behavior of the mass function in the chiral limit is a keystone of the microscopic realization of Goldstone’s theorem in QCD: the quark condensate (and hence the pion mass) and other observables are materially dependent on the ultraviolet properties of the interaction.

In the infrared region both the wave function renormalization  $Z(p^2) = 1/A(p^2)$  and the dynamical mass function deviate significantly from the perturbative behavior, due to chiral symmetry breaking. Recent comparisons [22, 23] of results from this rainbow DSE model to lattice QCD simulations [24] provide semiquantitative confirmation of the behavior generated by the present DSE model: a significant enhancement of  $M(p^2)$  and a material enhancement of  $A(p^2)$  below 1 GeV<sup>2</sup>.

The vector meson masses and electroweak decay constants produced by this model are in good agreement with experiments [9]. The model’s prediction for the pion charge form factor  $F_\pi(Q^2)$  is confirmed by the most recent Jlab data [25]. The kaon charge radii and electromagnetic form factors are also described well [10], as is the weak  $K_{l3}$  decay [11]. The strong decays of the vector mesons into a pair of pseudoscalar mesons also agree reasonably well with experiments [12, 26]. The performance of this model for deep inelastic scattering phenomena can be gauged from that of a simplified version that has recently produced reasonable results for the pion valence quark distribution amplitude [27].

### 3.2 Ground state mass spectrum of $q\bar{q}$ and $qq$ states

With this model we have calculated the masses of the lightest two-body bound states in the  $u, d, s$  quark sector: pseudoscalar, scalar, and vector mesons, and scalar, pseudoscalar, and axialvector diquarks. As far as the flavor-singlet mesons are concerned, with the rainbow-ladder kernel only flavor-singlet states with “ideal mixing” are possible. This feature indicates a deficiency of the rainbow-ladder truncation for studying flavor-singlet pseudoscalar and scalar mesons (the flavor-singlet vector mesons are very close to ideal mixing).

Regarding the flavor structure of the diquarks, the Pauli principle prohibits the existence of flavor-singlet color-antitriplet scalar and pseudoscalar diquarks; the only possible  $ss$  diquarks are axialvector diquarks [3, 16]. Nevertheless, in model studies such as this, one can consider the up/down quark masses to be equal to the strange quark mass, and calculate the corresponding meson and diquark masses. This indicates the dependence of the diquark masses on the current quark masses and allows for a comparison with other calculations. However, one should keep in mind that there are no scalar nor pseudoscalar  $ss$  diquarks in 3-flavor QCD with realistic quark masses.

The bound state BSE has solutions at discrete values of  $P^2 = -m^2$ , where  $m$  is the mass of the bound state. In order to determine the bound state masses, we introduce a parameter  $\lambda(P^2)$ , and turn the BSE into an eigenvalue problem

for  $\lambda(P^2)$

$$\frac{4}{3} \int_q^\Lambda \mathcal{G}(k^2) D_{\mu\nu}^{\text{free}}(k) \gamma_\mu S(q_+) \Gamma(q_+, q_-) S(q_-) \gamma_\mu = \lambda(P^2) \Gamma(p_+, p_-). \quad (17)$$

This equation has solutions for all  $P^2$ , but in general these solutions do not correspond to bound state solutions of the original BSE, Eqs. (9) and (10). Meson bound states with mass  $m$  are described by solutions of Eq. (17)  $\Gamma(p_+, p_-) = \Gamma_M(p_+, p_-)$  with  $\lambda(P^2 = -m^2) = 1$ , whereas diquark bound states are described by solutions  $\Gamma(p_+, p_-) = \Gamma_D(p_+, -p_-) C$  with  $\lambda(-m^2) = 2$  (remember that the color structure in the diquark BSE leads to a factor  $\frac{2}{3}$  instead of  $\frac{4}{3}$ , see Eq. (11)). In Fig. 3 we display the eigenvalues as function of  $P^2$  in the up/down sector. From this figure we can simply read of the values of  $P^2$  that give us the mass of a bound state.

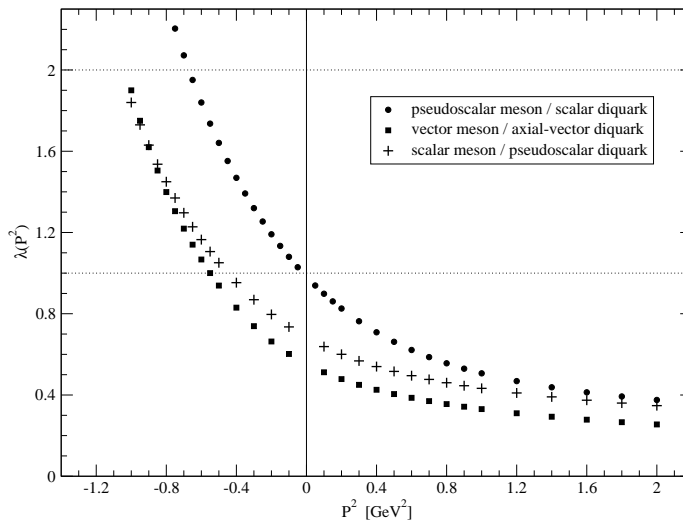


Figure 3: The eigenvalue  $\lambda(P^2)$  as function of  $P^2$  in the up/down sector:  $\lambda = 1$  signals a meson bound state, whereas  $\lambda = 2$  corresponds to a diquark bound state.

Since we started from a Euclidean formulation, we have to make an analytic continuation to negative values of  $P^2$  in order to determine the bound state solutions. For small masses, this is no problem; however, for larger masses this becomes numerically more and more cumbersome. Moreover, the quark propagator in rainbow truncation often has singularities at complex values of  $p^2$  [28], which could be interpreted as a signal for confinement [29]. Once the integration domain sampled in the BSE includes these singularities, one has to



specify how to deal with these singularities. Alternatively, one can extrapolate the eigenvalues  $\lambda(P^2)$  from the region where the analytic continuation is unambiguous to  $\lambda = 1$  for mesons, and to  $\lambda = 2$  for diquarks, whenever necessary. We followed the latter procedure, using several different extrapolating functions to reduce the numerical uncertainty. For the bound states with the largest mass, we estimate the error due to this extrapolation to be a few percent.

	$m_q = m_{q'} = m_{u,d}$			$m_q = m_{u,d}, m_{q'} = m_s$			$m_q = m_{q'} = m_s$		
meson	$\pi$	$\rho, \omega$	$\sigma$	$K$	$K^*$	$\kappa$	$0^-$	$\phi$	$0^+$
calc.	0.138	0.741	0.671	0.496	0.937	0.893	0.696	1.07	1.08
dom.	0.121	0.875	0.759	0.425	1.08	1.03	0.588	1.24	1.30
sep.	0.139	0.736	0.715	0.494	0.854	–		0.950	
lat.	0	0.579					0.910	1.025	
diquark	$0^+$	$1^+$	$0^-$	$0^+$	$1^+$	$0^-$	$0^+$	$1^+$	$0^-$
calc.	0.82	1.02	1.03	1.10	1.30(6)	1.31(4)	1.27	1.44(4)	1.50(4)
dom.	0.74	1.06	1.14(2)	0.94	1.34(4)	1.45(4)	1.12	1.51(4)	1.72(6)
sep.	0.74	0.95	1.50	0.88	1.05	–		1.13	
lat.	0.62	0.73					1.19	1.21	

Table 1: Overview of our results for the meson and diquark masses for different current quark masses, all in GeV, compared with the results from a separable model [30] and with quenched lattice QCD [5]. Note that the Pauli principle prohibits the existence of flavor-singlet color-antitriplet scalar and pseudoscalar diquarks; the results for the  $m_q = m_{q'} = m_s$  scalar and pseudoscalar diquark masses are only included to indicate the dependence on the current quark mass and for comparison with lattice data. Our numerical errors are of the order of 1%, with the exception of the heavier-mass states, which have an extrapolation error as indicated.

Our results are displayed in Table 1, and compared with results from rainbow-ladder truncation of the DSEs using a separable Ansatz for the interaction [30] and with lattice data [5] where available. Note that our calculation is done at realistic quark masses, whereas the lattice results are extrapolated to the chiral limit. For the strange quark we have taken the lattice data with  $m_V = m_\phi$ . Compared to the lattice data, we find a larger splitting between the scalar and the axialvector diquark; also in the  $s\bar{s}$  sector we find a significantly larger splitting between the pseudoscalar and vector meson. The lattice simulations do not report on scalar meson or pseudoscalar diquark masses.

Our results are qualitatively the same as the results of the separable model of Ref. [30], with the exception of the scalar mesons and pseudoscalar diquarks. We find the scalar and vector meson masses to be within 10% of each other, not only in the  $u/d$  sector, but also in the  $us$  and  $ss$  sectors. Similarly, we also find the pseudoscalar diquark and axialvector diquark masses to be within about 10% of each other, whereas in the separable model the pseudoscalar diquark is much heavier than the axialvector diquark, or not bound at all. Also notice that the scalar meson and pseudoscalar diquark masses increase more rapidly with the quark mass than the vector meson and scalar diquark masses: e.g. the  $m_\sigma < m_\rho$  but  $m_{0^+}^{s\bar{s}} > m_\phi$ .

In Table 1 we also give the masses obtained using only the dominant co-

variant for the different bound states; e.g., retaining only  $E$  in Eq. (3). This approximation changes the mass by about 20% both for the mesons and for the diquarks. Using the dominant covariants only tends to increase the difference between pseudoscalar meson masses and vector and scalar masses; we see a similar increase in the difference in the diquark channels.

The meson masses seem to be rather independent of the details of the effective interaction, as long as the interaction generates the observed amount of chiral symmetry breaking, as can be seen from Table 2. The parameters  $\omega$  and  $D$  were fitted in Ref. [9] to reproduce  $f_\pi$  and the chiral condensate. Within this parameter range, the vector meson masses are almost independent of the parameters, and the scalar meson masses change by only 10%. The diquark masses are more sensitive to details of the effective interaction. Nevertheless, the lightest diquark is the scalar diquark, independent of the parameters, with the axialvector and pseudoscalar diquarks being about 150 to 250 MeV heavier.

	mesons			diquarks		
	$\pi$	$\rho, \omega$	$\sigma$	$0^+$	$1^+$	$0^-$
$\omega = 0.3 \text{ GeV}, D = 1.25 \text{ GeV}^2$	0.139	0.746	0.669	0.98	1.1	1.2
$\omega = 0.4 \text{ GeV}, D = 0.93 \text{ GeV}^2$	0.138	0.741	0.671	0.82	1.02	1.03
$\omega = 0.5 \text{ GeV}, D = 0.79 \text{ GeV}^2$	0.138	0.742	0.596	0.688	0.89	0.86

Table 2: Parameter dependence of the masses (in GeV) in the up/down sector.

### 3.3 Bethe–Salpeter amplitudes

The corresponding BSAs are similar for the different bound states. In Fig. 4 we have displayed the leading Chebyshev moments

$$f(q^2) = \int_0^\pi \sin^2 \theta \, d\theta \, f(q^2, qP \cos \theta; \eta = \frac{1}{2}) \quad (18)$$

of the amplitudes associated with the canonical Dirac structure for the various mesons and diquarks in the up/down sector, all normalized to  $f(0) = 1$ :  $E$  for pseudoscalar and scalar bound states, see Eq. (3), and  $V_1$  for vector and axialvector bound states, see Eq. (4).

In the infrared region,  $0 < q^2 < 2 \text{ GeV}^2$ , the canonical covariants can reasonably well be approximated by exponentials  $f(q^2) = \exp(-q^2/\omega^2)$  with  $0.74 \text{ GeV} < \omega < 1.01 \text{ GeV}$ , depending on the meson or diquark, see Table 3. At large  $q^2$ , they all fall off like  $c/q^2$  up to calculable logarithmic corrections [8, 9]. It is thus apparent that in all three channels, the diquark BSAs are narrower in momentum space than the corresponding meson BSAs, and thus wider in coordinate space. This is what one would expect, since the diquarks are less bound. It is intriguing that the scalar meson BSA is broader in momentum space than the pion BSA, and thus narrower in coordinate space. One expects the *physical*  $\sigma$  state to include significant pion cloud contributions and to thus be

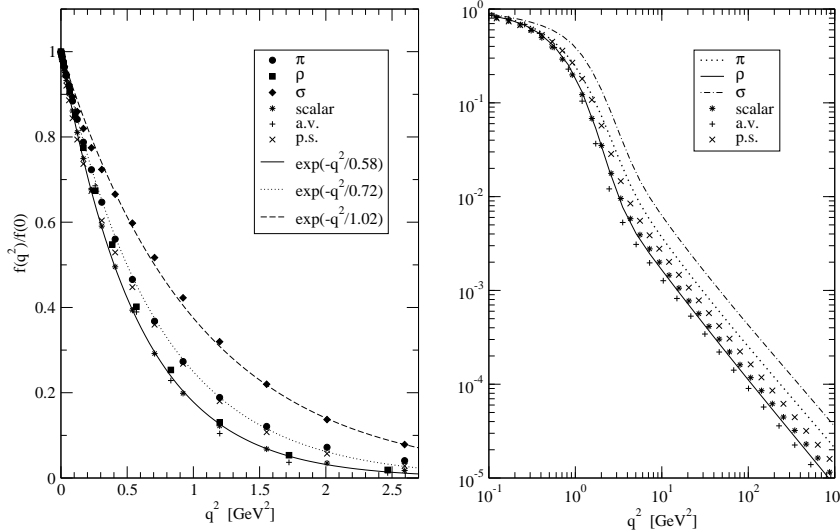


Figure 4: Leading Chebyshev moments of canonical amplitudes in the up/down sector.

state	mesons			diquarks		
	$\pi$	$\rho$	$\sigma$	$0^+$	$1^+$	$0^-$
$\omega$ [GeV]	0.84	0.79	1.01	0.76	0.74	0.82

Table 3: Comparison of the BSAs for the up/down states, fitted to  $\exp(-q^2/\omega^2)$  in the infrared region.

significantly broader in coordinate space than the pion. In ladder BSE approximation, such physical contributions are not accommodated; also other terms beyond rainbow-ladder truncation are known to be important in the scalar channel. Clearly, additional study beyond ladder truncation is required in the scalar channel.

## 4 Concluding remarks

We have calculated the meson and color-antitriplet diquark masses using DSEs in rainbow-ladder truncation. The model parameters have previously been fixed by the calculation of  $f_\pi$ ,  $m_\pi$ ,  $m_K$ , and the chiral condensate, and it leads to a good description of the light pseudoscalar and vector mesons and their interactions. Using this model, we find that the lightest diquark bound states in a color antitriplet configuration is a scalar diquark, with a mass of about

800 MeV in the case of up and down quarks. The axialvector and pseudoscalar diquarks are about 150 to 250 MeV heavier than the scalar diquark. In the meson channel, we find a scalar meson with a mass slightly below the vector meson for up/down quarks, but slightly above the vector meson mass for strange quarks. These results are consistent with the notion of a (broad)  $\sigma$ -meson with a mass around 600 MeV, and with the mass splitting between the scalar and vector mesons in heavy quarkonia. The corresponding BSAs are all similar in shape, and can in the infrared region be described by a gaussian. For large relative momenta, they fall off like  $1/p^2$ , with calculable logarithmic corrections which is characteristic of QCD.

The ladder truncation is particularly suitable for the pseudoscalar mesons and for the vector mesons, because of cancellations in the higher-order contributions to the kernel. However, diquarks, and also the scalar meson, are expected to receive significant corrections from higher order terms in the kernel. This can significantly change the bound state mass and corresponding BSA; in particular the diquarks will no longer be a true bound state. Thus one should only consider these masses as an indication for the relevant mass scales of the diquark correlations. As such they should be useful in e.g. studies of baryons as a quark-diquark system.

Typically, studies of baryons as a quark-diquark bound state include both scalar and axialvector diquarks in a color antitriplet, but no pseudoscalar diquarks. The present study indicates that the mass scale of pseudoscalar diquarks is similar to that of axialvector diquarks. It may therefore be interesting to explore the influence of pseudoscalar correlations on quark-diquark models for baryons such as those of Refs. [1, 2, 3, 4].

## Acknowledgements

I would like to thank Craig Roberts and Peter Tandy for useful discussions. This work is supported by DOE under grants No. DE-FG02-96ER40947 and DE-FG02-97ER41048 and benefitted from the computer resources at NERSC.

## References

- [1] R.T. Cahill, C.D. Roberts and J. Praschifka, Austral. J. Phys. **42**, 129 (1989); C.J. Burden, R.T. Cahill and J. Praschifka, Austral. J. Phys. **42**, 147 (1989).
- [2] H. Asami, N. Ishii, W. Bentz and K. Yazaki, Phys. Rev. C **51**, 3388 (1995); H. Mineo, W. Bentz and K. Yazaki, Phys. Rev. C **60**, 065201 (1999) [arXiv:nucl-th/9907043]; H. Mineo, W. Bentz, N. Ishii and K. Yazaki, arXiv:nucl-th/0201082.
- [3] M. Oettel, G. Hellstern, R. Alkofer and H. Reinhardt, Phys. Rev. C **58**, 2459 (1998) [arXiv:nucl-th/9805054]; M. Oettel, L. Von Smekal

- and R. Alkofer, *Comput. Phys. Commun.* **144**, 63 (2002) [arXiv:hep-ph/0109285]; R. Alkofer and M. Oettel, arXiv:hep-ph/0105320.
- [4] J. C. Bloch, C. D. Roberts, S. M. Schmidt, A. Bender and M. R. Frank, *Phys. Rev. C* **60**, 062201 (1999) [arXiv:nucl-th/9907120]; J. C. Bloch, C. D. Roberts and S. M. Schmidt, *Phys. Rev. C* **61**, 065207 (2000) [arXiv:nucl-th/9911068]; M. B. Hecht, M. Oettel, C. D. Roberts, S. M. Schmidt, P. C. Tandy and A. W. Thomas, arXiv:nucl-th/0201084.
- [5] M. Hess, F. Karsch, E. Laermann and I. Wetzorke, *Phys. Rev. D* **58**, 111502 (1998) [arXiv:hep-lat/9804023].
- [6] C. D. Roberts and S. M. Schmidt, *Prog. Part. Nucl. Phys.* **45S1**, 1 (2000) [arXiv:nucl-th/0005064].
- [7] R. Alkofer and L. von Smekal, *Phys. Rept.* **353**, 281 (2001) [arXiv:hep-ph/0007355].
- [8] P. Maris and C. D. Roberts, *Phys. Rev. C* **56**, 3369 (1997) [arXiv:nucl-th/9708029].
- [9] P. Maris and P. C. Tandy, *Phys. Rev. C* **60**, 055214 (1999) [arXiv:nucl-th/9905056].
- [10] P. Maris and P. C. Tandy, *Phys. Rev. C* **61**, 045202 (2000) [arXiv:nucl-th/9910033]; P. Maris and P. C. Tandy, *Phys. Rev. C* **62**, 055204 (2000) [arXiv:nucl-th/0005015].
- [11] C. Ji and P. Maris, *Phys. Rev. D* **64**, 014032 (2001) [arXiv:nucl-th/0102057].
- [12] P. Maris, arXiv:nucl-th/0112022.
- [13] P. Maris and P. C. Tandy, *Phys. Rev. C*, in press (2002) [arXiv:nucl-th/0201017].
- [14] R. T. Cahill, C. D. Roberts and J. Praschifka, *Phys. Rev. D* **36**, 2804 (1987).
- [15] M. B. Hecht, C. D. Roberts and S. M. Schmidt, *Lect. Notes Phys.* **578**, 218 (2001) [arXiv:nucl-th/0012023].
- [16] R. Alkofer and H. Reinhardt, *Berlin, Germany: Springer (1995) 114 p. (Lecture notes in physics)*.
- [17] A. Bender, W. Detmold, C. D. Roberts and A. W. Thomas, arXiv:nucl-th/0202082.
- [18] P. Maris, C. D. Roberts and P. C. Tandy, *Phys. Lett. B* **420**, 267 (1998) [arXiv:nucl-th/9707003].

- [19] A. Bender, C. D. Roberts and L. Von Smekal, Phys. Lett. B **380**, 7 (1996) [arXiv:nucl-th/9602012].
- [20] G. Hellstern, R. Alkofer and H. Reinhardt, Nucl. Phys. A **625**, 697 (1997) [arXiv:hep-ph/9706551].
- [21] F. T. Hawes, P. Maris and C. D. Roberts, Phys. Lett. B **440**, 353 (1998) [arXiv:nucl-th/9807056].
- [22] P. Maris, arXiv:nucl-th/0009064.
- [23] P. C. Tandy, arXiv:nucl-th/0106031.
- [24] J. Skullerud, D. B. Leinweber and A. G. Williams, Phys. Rev. D **64**, 074508 (2001) [arXiv:hep-lat/0102013].
- [25] J. Volmer *et al.* [The Jefferson Lab F(pi) Collaboration], Phys. Rev. Lett. **86**, 1713 (2001) [arXiv:nucl-ex/0010009].
- [26] D. Jarecke, P. Maris, and P. C. Tandy “Strong decays of light vector mesons,” in preparation, KSUCNR-101-01 (2002).
- [27] M. B. Hecht, C. D. Roberts and S. M. Schmidt, Phys. Rev. C **63**, 025213 (2001) [arXiv:nucl-th/0008049].
- [28] R. Fukuda and T. Kugo, Nucl. Phys. B **117**, 250 (1976); D. Atkinson and D. W. Blatt, Nucl. Phys. B **151**, 342 (1979); S. J. Stainsby and R. T. Cahill, Phys. Lett. A **146**, 467 (1990); P. Maris and H. A. Holties, Int. J. Mod. Phys. A **7**, 5369 (1992); P. Maris, Phys. Rev. D **50**, 4189 (1994).
- [29] C. J. Burden, C. D. Roberts and A. G. Williams, Phys. Lett. B **285**, 347 (1992); G. Krein, C. D. Roberts and A. G. Williams, Int. J. Mod. Phys. A **7**, 5607 (1992); P. Maris, Phys. Rev. D **52**, 6087 (1995) [arXiv:hep-ph/9508323].
- [30] C. J. Burden, L. Qian, C. D. Roberts, P. C. Tandy and M. J. Thomson, Phys. Rev. C **55**, 2649 (1997) [arXiv:nucl-th/9605027].